Are your MRI contrast agents cost-effective?
Learn more about generic Gadolinium-Based Contrast Agents.
FRESENIUS KABI
caring for life

AJNR

Combined Magnetization Transfer and Proton Spectroscopic Imaging in the Assessment of Pathologic Brain Lesions in Multiple Sclerosis

G. Bruce Pike, Nicola de Stefano, Sridar Narayanan, Gordon S. Francis, Jack P. Antel and Douglas L. Arnold

AJNR Am J Neuroradiol 1999, 20 (5) 829-837
http://www.ajnr.org/content/20/5/829

This information is current as of April 19, 2024.

AJNR Am J Neuroradiol 20:829–837, May 1999

Combined Magnetization Transfer and Proton Spectroscopic Imaging in the Assessment of Pathologic Brain Lesions in Multiple Sclerosis

G. Bruce Pike, Nicola de Stefano, Sridar Narayanan, Gordon S. Francis, Jack P. Antel, and Douglas L. Arnold

BACKGROUND AND PURPOSE: **Conventional MR imaging of multiple sclerosis (MS) provides relatively poor pathologic specificity, which has led to the investigation of more sophisticated MR techniques. The purpose of this study was to combine magnetization transfer (MT) imaging and proton MR spectroscopic imaging (MRSI) to evaluate the specific pathologic features of myelination and neuronal integrity in patients with MS and to determine the relationship between these measures within plaques.**

METHODS: **We acquired conventional MR, MT, and proton MRSI data and evaluated clinical disability in 30 patients with MS, whose conditions were categorized as relapsing-remitting, primary progressive, or secondary progressive. The lesions were classified, using a semiautomated edge-following technique, on T2-weighted MR images, and an analysis of MT and proton MRSI data was conducted for lesion regions as well as for tissue that was categorized as normal.**

RESULTS: **The MT ratio (MTR) of normal-appearing white matter in the patients with MS was significantly lower than in the healthy participants, whereas gray matter values were unchanged. MS lesions showed a large reduction in MTR, with old lesions exhibiting a lower MTR than new lesions. The average lesion MTR and the MR spectroscopic imaging–measured relative concentration of *N*-acetylaspartate, a marker of neuronal integrity, was positively correlated in patients with relapsing-remitting MS. This relationship was strengthened in regions containing new lesions.**

CONCLUSION: **The integrated use of MT and MR spectroscopic imaging provides a more complete description of the pathologic features of MS than does conventional MR imaging alone, and our data suggest that axonal damage occurs in step with new demyelination and is not a late feature of the disease.**

Conventional MR imaging, based primarily on T2-weighted images, has shown high detection sensitivity for multiple sclerosis (MS) but poor specificity in terms of differentiating the pathologic state of plaques (1–3). To address this shortcoming, a variety of MR techniques have been used in an attempt to detect or quantify pathologic aspects of MS. These techniques include, but are not limited to, hypointense T1-weighted lesion analysis for assessment tissue matrix destruction (4, 5), contrast-enhanced T1-weighted imaging to detect blood-brain barrier disruptions (6–9), multicomponent T2 quantitation to characterize various water compartments (10–12), diffusion imaging for structural change sensitivity (13, 14), spectroscopy for chemical profiling (15–20), and magnetization transfer (MT) imaging for measuring water-macromolecule interactions (21–27). In this study, we combined conventional MR lesion detection with MT and spectroscopic imaging.

The hydrogen nuclei of water are the main source of signal in conventional MR imaging because they exist in abundance, have high sensitivity, and possess relaxation times sufficiently long to permit easy detection. Macromolecular protons, such as those associated with the lipids of white matter, have extremely short T2 relaxation times ($<$ about 100 μs) and decay completely before they can be measured

Received November 6, 1998; accepted after revision January 22, 1999.

Supported by the Medical Research Council of Canada and Fonds de la Recherche en Santé du Québec. G.B.P., G.S.F., and D.L.A. are Killam Scholars; Philips Medical Systems provided their pulse sequence development environment.

From the McConnell Brain Imaging Center, Montreal Neurological Institute, McGill University, Canada (G.B.P., S.N., G.F., J.P.A., D.L.A.); and the Department of Neurology, University of Siena, Italy (N.D.S.).

Address reprint requests to Bruce Pike, PhD, Room WB-315, Montreal Neurological Institute, 3801 University St, Montreal, Quebec, Canada, H3A 2B4.

© American Society of Neuroradiology

with a conventional MR scanner. This population of semisolid hydrogen nuclei is thus effectively MR-invisible; however, magnetic interactions between the semisolid and water protons result in an exchange of magnetization between the two populations (28, 29). This MT process is probed in MT imaging by selectively saturating the semisolid component and observing the transfer of this saturation to the measured water pool (22, 30–33).

There are currently two primary roles of MT imaging in the assessment of MS. The first simply exploits the strong MT interactions in the CNS to suppress tissue signals while leaving contrast-enhanced signals unaffected, thereby improving the detectability of the enhancing lesions (34–39). The second attempts to quantify the extent of the MT interaction and thus indirectly to characterize the composition and structural integrity of white matter (21–25).

Although the exact mechanisms of MT in white matter are not definitively known and may involve many macromolecules, large, relatively immobile, lipids are thought to constitute the dominant interacting macromolecular component. Koenig (40) and Koenig et al (41) have suggested that the exchange occurs primarily between the cholesterol of myelin and surrounding myelin water and, via diffusion, axonal water. Ceckler et al (42) reported that sphingomyelin concentration and mobility play a more important role in determining MT than cholesterol. The most comprehensive in vitro analysis to date has been conducted by Kucharczyk et al (43), who studied all the major lipid components of white matter in a multilamellar vesicle model system. They observed that galactocerebroside had the greatest effect (per weight) on relaxivity and that MT was two to three times greater than with either cholesterol or sphingomyelin alone.

Water-suppressed proton MRSI measures hydrogen nuclei signals from various chemical compounds having relaxation times sufficiently long to allow detection but concentrations that are many orders of magnitude lower than water. Proton MRSI of normal human brain at late echo times (TE = 272) shows three major resonances: choline-containing compounds (Cho), creatine/phosphocreatine (Cr), and *N*-acetylaspartate (NAA). Two salient features of proton MRSI relevant to MS are that NAA is a neuronal marker (44–46) and that Cho signals arise from membrane components and increase with demyelination (47–49).

Multiple studies have shown that NAA resonance intensities are significantly decreased in chronic, irreversible plaques whereas acute lesions can show a transient decrease and then partial recovery (15, 17, 50, 51). Decreased NAA has also been observed in normal-appearing white matter, and thus, NAA has been proposed as a possible index of overall disease burden (48).

Previous MS studies that have evaluated the relationship between MT and NAA, as putative markers of myelination and neuronal integrity, respectively, have been limited to single-voxel MR spectroscopic acquisitions and have produced conflicting results (52, 53). We present the results of an analysis of 12 healthy subjects and 30 patients with MS with an MR protocol consisting of conventional MR, MT, and proton MRSI. Furthermore, previous serial conventional MR examinations of the patient group were used to establish lesion age. These data were analyzed by considering both average quantities per patient and voxel. The purpose of this study was to determine the relationship between the pathologic features of myelination and neuronal integrity within MS plaques.

Methods

After obtaining approval from our institutional review board and informed consent from each study participant, we collected T1-, T2-, and proton density–weighted MR, MT, and proton MRSI data from 12 healthy volunteers and 30 patients with MS. In all patients, clinical disability was evaluated at the time of the MR examination using the Kurtzke expanded disability status scale (EDSS) (54). Clinical subgroups (relapsing-remitting, 11 patients; primary progressive, five patients; and secondary progressive, 14 patients) were defined according to standard criteria (55). The relapsing-remitting subgroup consisted of five women and six men, 33 ± 6 (mean ± SD) years old, who had an EDSS range of 3 through 7 (5 ± 1); the primary progressive subgroup consisted of one woman and four men, 45 ± 10 years old, with an EDSS range of 4 through 7 (6 ± 1); and the secondary progressive subgroup consisted of five women and nine men, 50 ± 8 years old, with an EDSS range of 4 through 8 (6 ± 1). The healthy volunteers were 31 ± 7 years old and consisted of five women and seven men.

All MR data were acquired using a 1.5-T scanner in oblique axial planes parallel to the anterior-posterior commissure line and landmarked on the superior margin of the corpus callosum. A multisection, dual-echo, spin-echo sequence of 2100/30,80 (TR/TE_1, TE_2) with a section thickness of 5.5 mm, a section gap of 0.5 mm, and 20 sections was used to acquire proton density- and T2-weighted images.

T1-weighted and MT images were obtained using a pair of spin-echo acquisitions, without (No Sat) and with (Sat) MT saturation pulses, respectively, and parameters of 1000/20. Semisolid spin saturation was achieved using 1.2-millisecond on-resonance $1\bar{2}1$ binomial pulses ($|B_1| = 20\ \mu T$) placed just before each section-selective excitation (22). Twenty sections, coincident with the T2- and proton density-weighted images, were excited per repetition, thus rendering an effective saturation repetition period of 50 milliseconds. The percentage of difference (100 × [No Sat − Sat]/No Sat) MT ratio (MTR) images were calculated after thresholding above the noise background.

Proton MRSI was performed using a volume-selective, inversion-recovery water-suppressed, 90°–180°–180° (PRESS) sequence (56) with parameters of 2000/272. The selected volume of interest, measuring approximately 100 mm anteroposterior × 20 mm inferosuperior × 90 mm left-right, was centered on the corpus callosum and acquired using a 32 × 32 matrix, a 250-mm field of view, and one signal average, thus producing a voxel volume of 1.2 cm^3. With reconstruction filtering, the effective in-plane resolution was 1.2 cm. To correct for static and dynamic field inhomogeneities, these data were normalized by a second data set acquired without water suppression (850/272 and a 16 × 16 matrix) (57). MR spectroscopy postprocessing and quantitation were performed using a combination of SunSpec1 (Philips Medical Systems, Best, The Netherlands) and locally developed software. NAA/Cr images were calculated and interpolated (nearest-neighbor) onto a vol-

Acquisition parameters for the imaging protocol

	PDW/T2W	T1W/MT-No Sat	MT-Sat	MRSI
Sequence	Dual-echo SE	SE	SE with MT pulse*	PRESS
TR (ms)	2010	940	940	2000
TE (ms)	30/80	20	20	272
FOV (mm)	250 (80%)	250 (70%)	250 (70%)	250
Sections	20	20	20	1
Thickness (mm)	5.5	5.5	5.5	20
Section gap (mm)	0.5	0.5	0.5	—
Matrix	256 × 256	256 × 256	256 × 256	32 × 32
Scan time (min:sec)	6:56	2:55	2:55	34:08

Note: PDW indicates proton density—weighted; T2W, T2-weighted; T1W, T1-weighted; MT, magnetization transfer; No Sat, without MT saturation pulses; Sat, with MT saturation pulses; MRSI, MR spectroscopic imaging; FOV, field of view; SE, spin-echo.

* A 1.2-millisecond on-resonance $\overline{121}$ pulse with $|B_1| = 20\ \mu T$ was used in the MT saturation sequence.

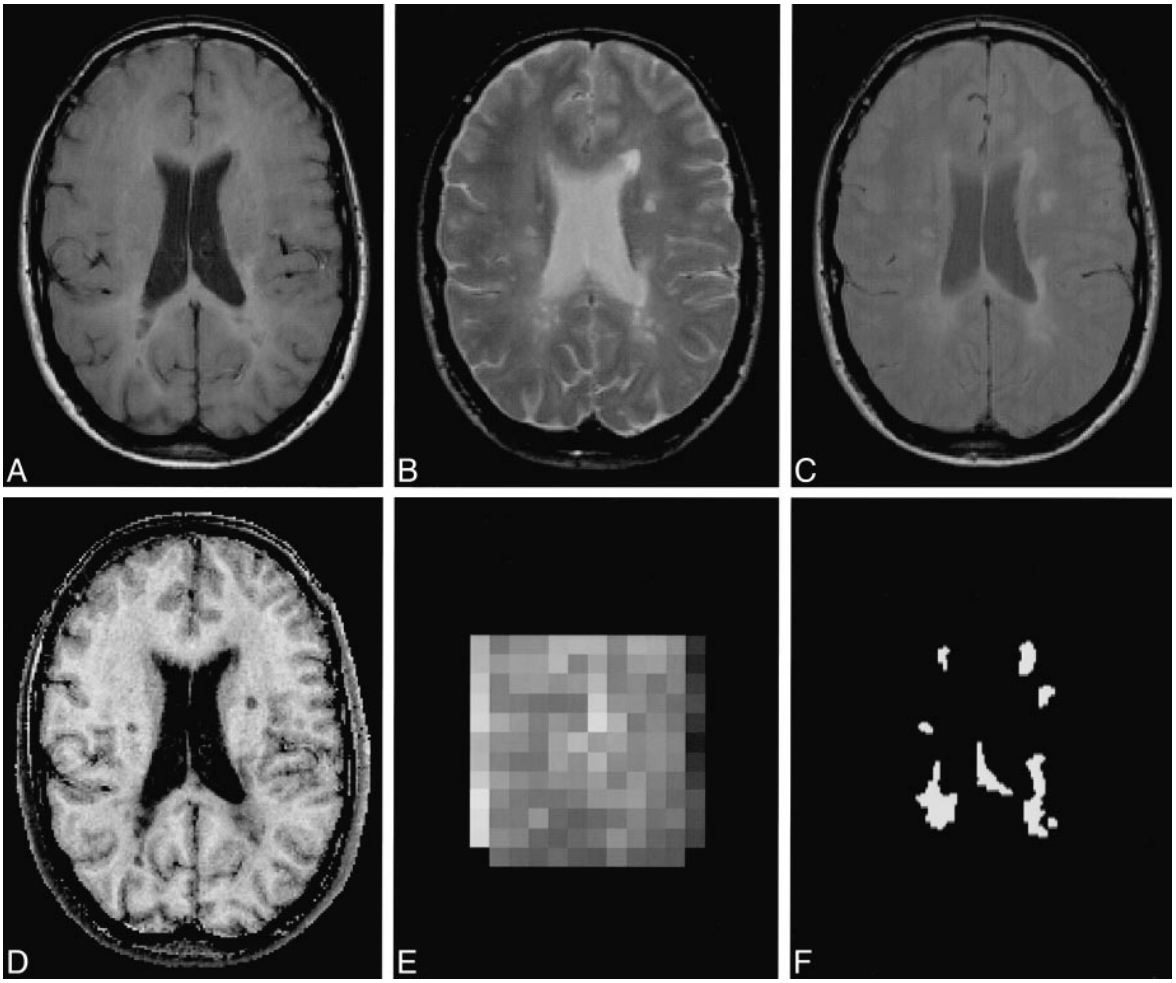

FIG 1. *A–F,* T1-weighted (*A*), T2-weighted (*B*), proton density–weighted (*C*), MTR (*D*), and NAA/Cr (*E*) spectroscopic images of a patient with MS acquired using the protocol presented in the Table; also shown is the classified lesion map for this section (*F*).

umetric matrix matching the MR data. Cr for normalization is widely used and permits comparisons with other published results. Although Cr fluctuation within lesions may occur (58–60), recent studies have shown that Cr decreases only transiently in acute lesions and subsequently returns to a stable baseline (51). Changes in Cr should therefore not significantly affect overall observations and trends in patients with chronic MS.

In addition to the cross-sectional data acquired as described above, serial MR (proton density— and T2-weighted) data from four previous examinations, performed approximately 6 months apart, were available for analysis. The complete acquisition protocol is summarized in the Table. Figure 1 shows a typical data set, with panels A, B, and C corresponding to conventional T1-, T2-, and proton density–weighted images,

respectively. Figure 1D shows the percent difference MTR image of the same section, and Figure 1E is the corresponding spectroscopic image of NAA/Cr. Figure 1F is the lesion map derived from the T2- and proton density–weighted images (panels B and C) using the algorithm described below.

A semiautomated tissue segmentation and analysis package (61) was used by one experienced expert to classify all MS lesions and the ventricles as seen on T2- and proton density–weighted images. Lesions defined by all previous MR examinations were transferred to the current time point using a coordinate transformation matrix determined by an automated registration of the previous and current proton density–weighted image volumes (62). This permitted all lesion voxels to be classified as new (those identified as normal by all previous examinations; ie, <6 months old) or old (those identified as lesions by all previous examinations; ie, >24 months old). Lesion voxels with an intermediate age and those with classifications that varied between lesion and normal were not included in this analysis. Regions of interest (ROIs) were also manually defined in four white matter areas (frontal, occipital, and genu and splenium of the corpus callosum) and four gray matter areas (frontal and occipital cortical, head of the caudate nucleus, and putamen) in the volunteers and in normal-appearing tissue (ie, outside all identified lesions but as close as possible to the areas selected in the volunteers) in the patients with MS. MTR values from lesions and normal-appearing white matter ROIs for patients with MS, clinical subgroups, and healthy subjects were compared using Student's *t*-test and correlated with lesion volume, MR spectroscopic data, and EDSS scores. All quantities averaged per patient were analyzed using Spearman rank correlation, whereas Pearson linear correlation analysis was used for all voxel-based data.

Results

From the manual ROI analysis of the healthy subjects, we measured MTR values of 41.3 ± 1.4% for white matter and 28.5 ± 1.7% for gray matter. MTR values were highest in the genu of the corpus callosum (42.6 ± 1.3%) and were next highest in the splenium of the corpus callosum (41.4 ± 1.2%), frontal white matter (41.3 ± 1.1%), and occipital white matter (40.0 ± 0.8%). These regions were all significantly different from one another ($P < .05$) except for the frontal white matter and the splenium of the corpus callosum. In gray matter, MTR was higher in the putamen (30.1 ± 1.2%) than in the other regions (28.0 ± 1.5%), which were not significantly different from one another.

In the patients with MS, MTR in normal-appearing white matter was slightly, but significantly, decreased to 38.3 ± 2.4% ($P < .0001$), whereas gray matter MTR was unchanged at 28.1 ± 2.9% ($P = .4$). Similar observations also held for each patient subgroup. No significant differences between normal-appearing white matter MTRs for the relapsing-remitting (38.0 ± 21.%), primary progressive (38.3 ± 1.8%), and secondary progressive (38.1 ± 2.7%) subgroups were observed.

In the patients with MS, the intra- and interlesional variation in MTR was large (range, about 5% to 40%). The range of average lesion MTR values across patients was 18.8% to 30.7%, for a mean value of 26.9 ± 2.6% that was significantly lower than white matter in the healthy subjects ($P < .0001$) and in the normal-appearing white matter in the MS patients ($P < .0001$). Average lesion MTR was not significantly different among the subgroups (lesion volume was 43.3 ± 22.9, 20.3 ± 8.4, and 26.0 ± 14.7 cm^3 for the relapsing-remitting, primary progressive, and secondary progressive subgroups, respectively). With respect to lesion age, MTR was significantly ($P < .0001$) lower in old lesion voxels (24.6 ± 3.6%, lesion volume = 7.6 cm^3) than in new ones (28.4 ± 2.7%, lesion volume = 5.6 cm^3). This difference held for all patient subgroups. Spearman rank correlation analysis of the entire MS cohort and each subgroup indicated that neither total lesion volume nor average lesion MTR or NAA/Cr were significantly correlated with the EDSS-based clinical assessment.

To assess the relationship between MTR and NAA/Cr, we conducted correlation analyses on average values for all lesions per patient and average value per voxel of the MRSIs. The results of the patient-based analyses are shown in Figures 2 and 3 for all lesions and for new lesions, respectively. Considering, first, all lesions in all patients (Fig 2A), no significant correlation was detected, yet a weak positive trend seemed apparent. In the relapsing-remitting subgroup, a significant positive correlation was observed (Spearman rank correlation coefficient, r_S, = .7, $P = .016$). No correlations were detected in the primary progressive or secondary progressive subgroups. Restricting the focus to new lesion voxels enhanced the coupling between MTR and NAA/Cr (Fig 3) for both the entire MS cohort ($r_S = .44$, $P = .032$) and the relapsing-remitting subgroup ($r_S = .81$, $P = .002$) but did not reveal correlations in the primary progressive or secondary progressive subgroups.

The voxel-based correlation analyses were conducted at the spectroscopic imaging resolution in all voxels containing more than 25% lesion and less than 10% ventricle, as defined by the semiautomated segmentation process. These values were empirically chosen to include as many lesion-containing MRSI voxels as possible while minimizing partial volume with the ventricles. For the entire patient group, a weak positive correlation (Pearson linear correlation coefficient, r_P, = .27, $P < .0001$) was then observed (Fig 4A). As with the patient-based analysis, the correlation was stronger ($r_P = .45$, $P < .0001$) for the relapsing-remitting subgroup (Fig 4B) and was not present for the primary progressive and secondary progressive subgroups.

Discussion

The pathologic heterogeneity of MS lesions is not well characterized using conventional T2- and proton density–weighted MR imaging. On the other hand, NAA/Cr as measured by MTR and MRSI, more closely reflects the pathologically important features of myelination and neuronal integrity, respectively. The combination of these techniques constitutes a powerful means of studying the nat-

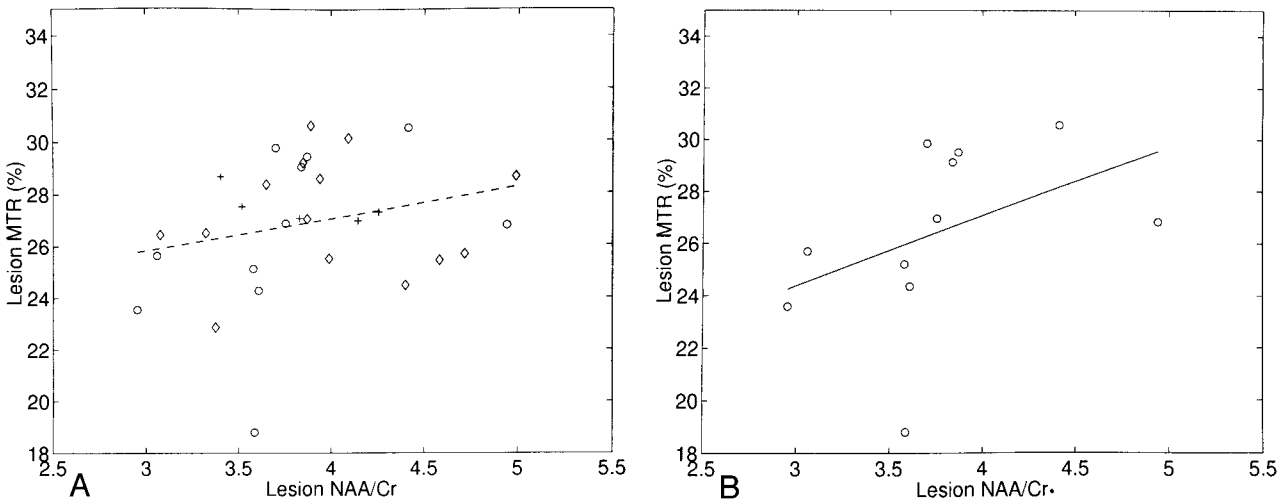

FIG 2. *A* and *B,* Mean (per patient) lesional MTR versus NAA/Cr for the entire cohort of patients with MS (*A*) and the relapsing-remitting subgroup (*B*) (*circles* indicate relapsing-remitting group; *plus signs,* primary progressive; *diamonds,* secondary progressive). Linear regression lines are plotted for both data sets, but the correlation was significant only for the relapsing-remitting subgroup (*solid line* in *B*; $r_s = .70$; $P = .016$).

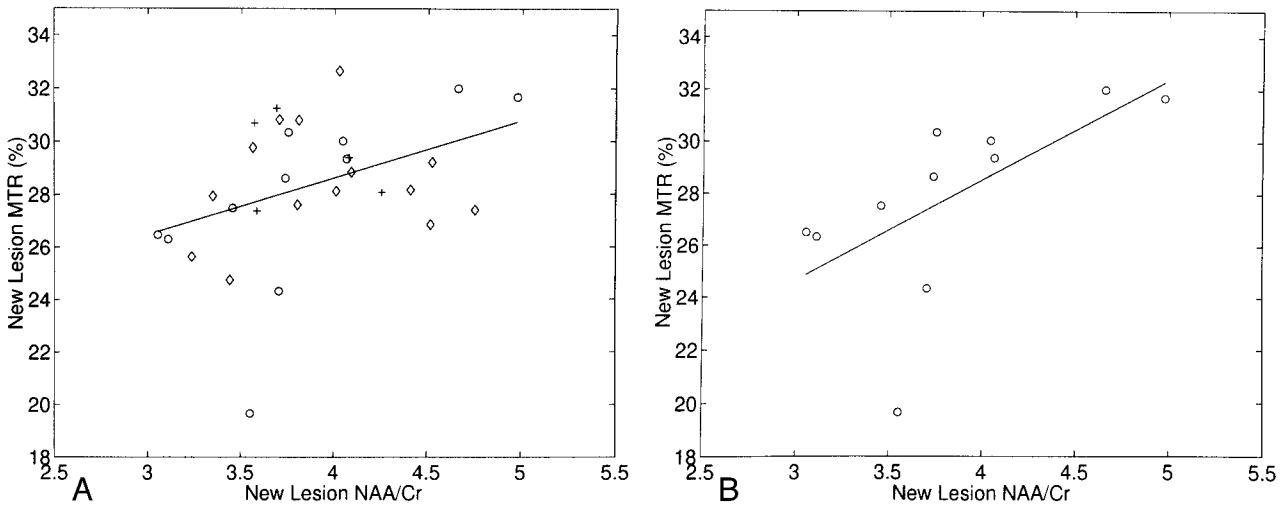

FIG 3. *A* and *B,* Mean (per patient) MTR versus NAA/Cr in new lesions (<6 months old) for the entire cohort of patients with MS (*A*) and the relapsing-remitting subgroup (*B*) (*circles* indicate relapsing-remitting group; *plus signs,* primary progressive; *diamonds,* secondary progressive). The *solid lines* represent the linear regressions, and the corresponding rank correlations were $r_s = .44$, $P = .015$ (*A*) and $r_s = .81$, $P = .002$ (*B*).

ural history of MS and assessing the effects of various therapeutic agents, and may therefore have an important role in clinical radiology.

Data obtained from our healthy subjects indicated that measures of the percentage of MTR were very consistent across subjects, with the manually defined white matter distribution having a standard deviation (SD) of less than 1.5%. The statistically significant differences between various white matter regions most likely occurred because of known differences in water content, fiber density, myelination, or in all three. Our observation of decreased MTR in the normal-appearing white matter of patients with MS has also been reported by others and has been hypothesized to be the result of microscopic lesions not directly visible on conventional MR images (21, 27, 63, 64). The small decrease in MTR might, however, also result from wallerian degeneration remote from the observed focal lesions (65) or molecular pathology related to other, as yet undefined, mechanisms. Mehta et al (66) examined a large number of healthy volunteers with a wide age range and found no correlation between the age of the subject and MTR, thus eliminating age as a possible explanation of the observation. That the difference between white matter in healthy subjects and normal-appearing white matter in patients with MS is significant for all the regions considered favors a hypothesis involving widespread white matter involvement.

The known pathologic heterogeneity of MS lesions can account for the large range of observed MTR values. It is likely that lesions with almost no MT (MTR < about 10%) represent very severe

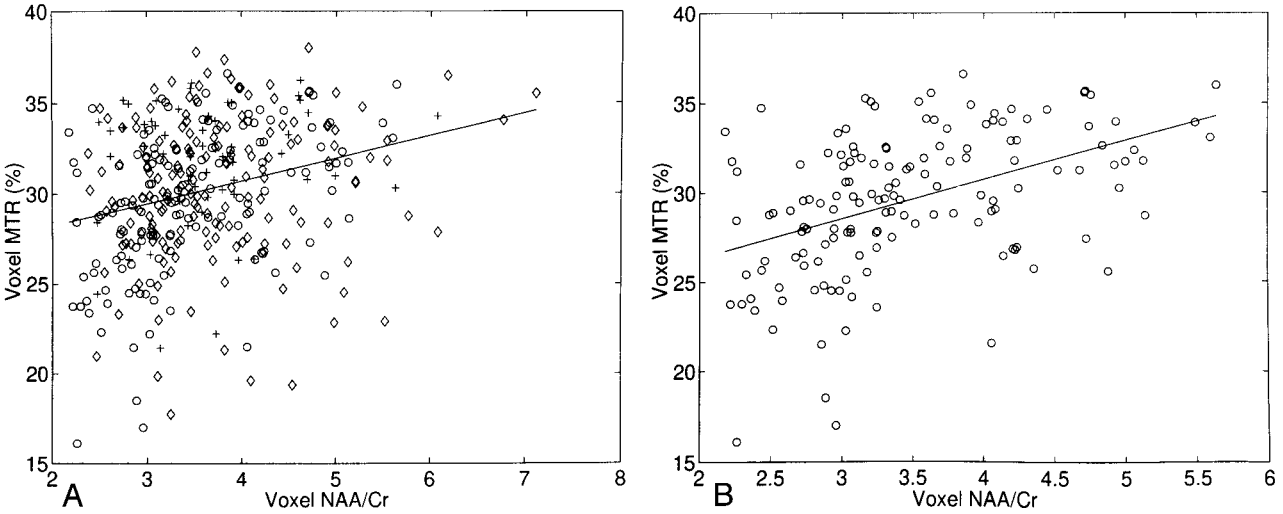

FIG 4. *A* and *B*, Mean (per MRSI voxel) MTR versus NAA/Cr in all MRSI voxels containing more than 25% lesion and less than 10% ventricle for the entire cohort of patients with MS (*A*) and the relapsing-remitting subgroup (*B*) (*circles* indicate relapsing-remitting group; *plus signs,* primary progressive; *diamonds,* secondary progressive). The *solid lines* represent the linear regressions corresponding to linear correlations of $r_P = .27$, $P < .0001$ (*A*) and $r_P = .45$, $P < .0001$ (*B*).

tissue destruction that results in open fluid-filled spaces corresponding to the ''open'' lesions described by Barnes et al (67). These lesions appear hyperintense on T2-weighted images and hypointense on T1-weighted images, which is consistent with a liquid. The extent to which these lesions contain viable axons, despite extensive demyelination, is not apparent from MT data alone and is better addressed by the MRSI measures of NAA. Although the limited spatial resolution of MR spectroscopy makes it difficult to completely isolate such dramatic focal MT abnormalities, our analyses indicate that spectroscopic lesion voxels with the lowest range of MTRs also have very low NAA/Cr (Fig 4).

As in the case of normal-appearing white matter, lesions with a mildly low MTR (about 35% to 40%) may represent edema only or a combination of edema and slight demyelination. This conclusion is supported by the work of Dousset et al who showed, using an animal model of acute experimental allergic encephalomyelitis, that edematous lesions, with essentially no histologically detectable demyelination, experienced only small decreases (about 5% to 8%) in MTR, whereas the plaques of clinically definite MS patients showed a much larger reduction (21). Therefore, plaques with an intermediate MTR (about 10% to 30%) likely have varying degrees of demyelination. The results presented by Hiehle et al (52), who found a strong inverse correlation between MTR and short-TE proton MRSI marker peaks, which they suggest originate from myelin degradation products, also support this hypothesis.

The observation of significantly lower MTR in old versus new lesions suggests increased demyelination with lesion age and hence a high prevalence of chronic activity in lesions. Note, however, that no difference was detected among patient subgroups. A more complete analysis of the temporal behavior of MTR in these patients, based on additional follow-up examinations, supports this observation of MTR decline with lesion age (68).

Previous studies have shown relatively weak (23, 69–71) or no correlation between T2-weighted lesion volume and clinical disability as assessed by EDSS. The primary factors that most likely contribute to this result are spinal cord disease (which was not measured in this study), the pathologic heterogeneity of T2-weighted lesions that are classified as equivalent, the presence of T2-weighted lesions in relatively silent brain regions that do not have a significant impact on EDSS, and the nonlinear and complex nature of the EDSS assessment (3). The issue of spinal cord lesions could be addressed by a more complete examination that encompasses this anatomic region. However, the problem of pathologic heterogeneity indicates that additional data, such as those available from MTR and MRSI, are required to measure the more specific tissue characteristics of demyelination and axonal loss that are the substrates of clinical disability. Possible deficiencies in the EDSS measure might be addressed by focusing correlation analyses on specific neurologic deficits and corresponding functional regions (eg, motor impairment and corticospinal tract lesion load) or, alternatively, by incorporating more comprehensive assessments of other parameters, such as cognitive impairment in a more encompassing clinical rating.

The interpretation of the absence of correlation between T2-weighted lesion volume and clinical disability observed in this study is further complicated by the highly nonuniform distribution of EDSS values (5.7 ± 1.2) in our patient group. In the secondary progressive subgroup, for example, all patients had an EDSS score of 6.0 or 6.5 with the exception of two, whose EDSS ratings were 4.0

and 8.0 (6.3 ± 0.82). These conditions are suboptimal for detecting any correlation, particularly one that is already expected to be weak. This may also explain, at least in part, the failure to find a significant correlation between average lesion MTR and EDSS, which has been reported previously (23). In the relapsing-remitting subgroup, whose EDSS variation was the greatest (4.95 ± 1.35), a general negative trend of decreased lesion MTR with increased disability was observed, but there was at least one major exception. The patient with the lowest average lesion MTR (18.8%, approximately 2 SD below the mean of the entire patient cohort) had an EDSS of only 4.5. This was not an artifactual observation resulting from a highly destructive small plaque, because the patient's lesion volume was substantial (49.7 cm^3) and well within the distribution of the group (31.3 ± 19.3 cm^3). Instead, this patient's case is perhaps demonstrative of two concerns. The first is the potential pitfalls of using the EDSS in such correlation analyses, because the patient's motor abilities were only mildly affected whereas he suffered considerable cognitive disabilities. The second is the importance of factors other than demyelination (eg, axonal loss) in determining disability.

An additional confounding problem is that the MTR techniques that show the percentage of difference provide only semiquantitative images that reflect a complex combination of sequence and relaxation parameters in addition to cross-relaxation terms (22, 33). The development of a truly quantitative MT imaging method, similar to the in vitro technique developed by Henkelman et al (72), would provide explicit measures of the liquid and semisolid pool sizes, individual relaxation times, and cross-relaxation rate. These data could provide considerably more specificity in interpreting MTR measures and would also provide a more appropriate basis for comparisons among sites.

NAA is now a well-established marker of neuronal functional and structural integrity. Because, in general, we expect a pathophysiologic correlation between demyelination and neuronal damage in association with MS, we hypothesized and observed correlations between MTR and spectroscopic imaging measures of NAA/Cr. Previous single-voxel MR spectroscopic studies have produced conflicting results. Hiehle et al (52) observed no correlation between NAA and MTR in a study of 11 patients, and Kimura et al (53) found a strong correlation (r_P = .73) in a group of 13 patients. Using spectroscopic imaging, which allows the simultaneous assessment of a large number of relatively small brain voxels, we were able to show that the degree of correlation is heavily dependent on lesion age. In addition, our results show a variable degree of correlation that is dependent on the patient subgroup. Acute lesions, which are more likely to be present in cases of relapsing-remitting MS, are known to be associated with large reversible decreases in NAA (50), edema, and active demyelination that is, in part, reversible. Consistent with this, our results indicated a closer coupling between MTR and NAA/Cr in patients in the relapsing-remitting subgroup rather than in the primary progressive and secondary progressive subgroups and further stronger coupling in new active lesions.

Conclusion

Using a protocol consisting of conventional MR, MT, proton spectroscopic imaging, and clinical evaluation, we conducted a cross-sectional study of 30 patients with MS and 12 healthy subjects. We observed widespread MT abnormalities in the normal-appearing white matter of the patients with MS, indicating disease activity beyond the boundaries of conventional MR-defined lesions. For the entire MS group, a weak correlation was detected between the putative markers of demyelination (MTR) and neuronal dysfunction (NAA/Cr). The coupling between these parameters was considerably stronger for the patients with relapsing-remitting conditions and for new lesions, suggesting that axonal damage occurs in step with new demyelination and is not a late feature of the disease. The combined use of conventional MR, MT, and MRSI provides a view of MS lesion disease that is more complete than that provided by any one method alone.

Acknowledgments

We thank Paul Matthews for many stimulating discussions, and Alan Evans for providing registration software.

References

1. Wallace CJ, Seland TP, Fong TC. **Multiple sclerosis: the impact of MR imaging.** *AJR Am J Roentgenol* 1992;158:849–857
2. Miller DH. **Magnetic resonance in monitoring the treatment of multiple sclerosis.** *Ann Neurol* 1994;36:S91–S94
3. Miller DH, Grossman RI, Reingold SC, McFarland HF. **The role of magnetic resonance techniques in understanding and managing multiple sclerosis.** *Brain* 1998;121:3–24
4. Truyen L, van Waesberghe JH, van Walderveen MA, et al. **Accumulation of hypointense lesions ("black holes") on T1 spin-echo MRI correlates with disease progression in multiple sclerosis.** *Neurology* 1996;47:1469–1476
5. van Walderveen MA, Kamphorst W, Scheltens P, et al. **Histopathologic correlate of hypointense lesions on T1-weighted spin-echo MRI in multiple sclerosis.** *Neurology* 1998;50:1282–1288
6. Valk J, de Slegte RG, Crezee FC, Hazenberg GJ, Thjaha SI, Nauta JJ. **Contrast enhanced magnetic resonance imaging of the brain using gadolinium-DTPA.** *Acta Radiol* 1987;28:659–665
7. Miller DH, Barkhof F, Nauta JJ. **Gadolinium enhancement increases the sensitivity of MRI in detecting disease activity in multiple sclerosis.** *Brain* 1993;116(Pt 5):1077–1094
8. Frank JA, Stone LA, Smith ME, Albert PS, Maloni H, McFarland HF. **Serial contrast-enhanced magnetic resonance imaging in patients with early relapsing-remitting multiple sclerosis: implications for treatment trials.** *Ann Neurol* 1994; 36(Suppl):S86–S90
9. Filippi M, Campi A, Martinelli V, et al. **Comparison of triple dose versus standard dose gadolinium-DTPA for detection of MRI enhancing lesions in patients with primary progressive multiple sclerosis.** *J Neurol Neurosurg Psychiatry* 1995;59: 540–544

10. Armspach JP, Gounot D, Rumbach L, Chambron J. **In vivo determination of multiexponential T2 relaxation in the brain of patients with multiple sclerosis.** *Magn Reson Imaging* 1991;9:107–113
11. MacKay A, Whittall K, Adler J, Li D, Paty D, Graeb D. **In vivo visualization of myelin water in brain by magnetic resonance.** *Magn Reson Med* 1994;31:673–677
12. Vavasour IM, Whittall KP, MacKay AL, Li DKB, Vorobeychik G, Paty DW. **A comparison between magnetization transfer ratios and myelin water percentages in normals and multiple sclerosis patients.** *Magn Reson Med* 1998;40:763–768
13. Christiansen P, Gideon P, Thomsen C, Stubgaard M, Henriksen O, Larsson HB. **Increased water self-diffusion in chronic plaques and in apparently normal white matter in patients with multiple sclerosis.** *Acta Neurol Scand* 1993;87:195–199
14. Horsfield MA, Larsson HB, Jones DK, Gass A. **Diffusion magnetic resonance imaging in multiple sclerosis.** *J Neurol Neurosurg Psychiatry* 1998;64:S80–S84
15. Wolinsky JS, Narayana PA, Fenstermacher MJ. **Proton magnetic resonance spectroscopy in multiple sclerosis.** *Neurology* 1990;40:1764–1769
16. Grossman RI, Lenkinski RE, Ramer KN, Gonzalez-Scarano F, Cohen JA. **MR proton spectroscopy in multiple sclerosis.** *AJNR Am J Neuroradiol* 1992;13:1535–1543
17. Davie CA, Hawkins CP, Barker GJ, et al. **Serial proton magnetic resonance spectroscopy in acute multiple sclerosis lesions.** *Brain* 1994;117(Pt 1):49–58
18. Hirsch JA, Lenkinski RE, Grossman RI. **MR spectroscopy in the evaluation of enhancing lesions in the brain in multiple sclerosis.** *AJNR Am J Neuroradiol* 1996;17:1829–1836
19. Arnold DL, Wolinsky JS, Matthews PM, Falini A. **The use of magnetic resonance spectroscopy in the evaluation of the natural history of multiple sclerosis.** *J Neurol Neurosurg Psychiatry* 1998;64:S94–S101
20. De Stefano N, Matthews PM, Fu L, et al. **Axonal damage correlates with disability in patients with relapsing-remitting multiple sclerosis: results of a longitudinal magnetic resonance spectroscopy study.** *Brain* 1998;121:1469–1477
21. Dousset V, Grossman RI, Ramer KN, et al. **Experimental allergic encephalomyelitis and multiple sclerosis: lesion characterization with magnetization transfer imaging.** *Radiology* 1992;182:483–491
22. Pike GB, Glover GH, Hu BS, Enzmann DR. **Pulsed magnetization transfer spin-echo MR imaging.** *J Magn Reson Imaging* 1993;3:531–539
23. Gass A, Barker GJ, Kidd D, et al. **Correlation of magnetization transfer ratio with clinical disability in multiple sclerosis.** *Ann Neurol* 1994;36:62–67
24. Mehta RC, Pike GB, Enzmann DR. **Measure of magnetization transfer in multiple sclerosis demyelinating plaques, white matter ischemic lesions, and edema.** *AJNR Am J Neuroradiol* 1996;17:1051–1055
25. van Buchem MA, Udupa JK, McGowan JC, et al. **Global volumetric estimation of disease burden in multiple sclerosis based on magnetization transfer imaging.** *AJNR Am J Neuroradiol* 1997;18:1287–1290
26. Petrella JR, Grossman RI, McGowan JC, Campbell G, Cohen JA. **Multiple sclerosis lesions: relationship between MR enhancement pattern and magnetization transfer effect.** *AJNR Am J Neuroradiol* 1996;17:1041–1049
27. Filippi M, Rocca MA, Martino G, Horsfield MA, Comi G. **Magnetization transfer changes in the normal appearing white matter precede the appearance of enhancing lesions in patients with multiple sclerosis.** *Ann Neurol* 1998;43:809–814
28. Edzes HT, Samulski ED. **The measurement of cross-relaxation effects in the proton NMR spin-lattice relaxation of water in biological systems: hydrated collagen and muscle.** *J Magn Reson* 1978;31:207–229
29. Fung B. **Nuclear magnetic resonance study of water interactions with proteins, biomolecules, membranes, and tissues.** In: Packer L, ed. *Methods in Enzymology*. San Diego: Academic Press; 1986;127:151
30. Wolff SD, Balaban RS. **Magnetization transfer contrast (MTC) and tissue water proton relaxation in vivo.** *Magn Reson Med* 1989;10:135–144
31. Hu BS, Conolly SM, Wright GA, Nishimura DG, Macovski A. **Pulsed saturation transfer contrast.** *Magn Reson Med* 1992;26:231–240
32. Yeung HN, Aisen AM. **Magnetization transfer contrast with periodic pulsed saturation.** *Radiology* 1992;183:209–214
33. Pike GB. **Pulsed magnetization transfer contrast in gradient echo imaging: a two-pool analytic description of signal response.** *Magn Reson Med* 1996;36:95–103
34. Tanttu JI, Sepponen RE, Lipton MJ, Kuusela T. **Synergistic enhancement of MRI with GdDTPA and magnetization transfer.** *J Comput Assist Tomogr* 1992;16:19–24
35. Mehta RC, Pike GB, Haros SP, Enzmann DR. **Central nervous system tumor, infection, and infarction: detection with gadolinium-enhanced magnetization transfer MR imaging.** *Radiology* 1995;195:41–46
36. Elster AD, Mathews VP, King JC, Hamilton CA. **Improved detection of gadolinium enhancement using magnetization transfer imaging.** *Neuroimaging Clin N Am* 1994;4:185–192
37. Mathews VP, Elster AD, King JC, Ulmer JL, Hamilton CA, Strottmann JM. **Combined effects of magnetization transfer and gadolinium in cranial MR imaging and MR angiography.** *AJR Am J Roentgenol* 1995;164:169–172
38. van Waesberghe JH, Castelijns JA, Roser W, et al. **Single-dose gadolinium with magnetization transfer versus triple-dose gadolinium in the MR detection of multiple sclerosis lesions.** *AJNR Am J Neuroradiol* 1997;18:1279–1285
39. Silver NC, Good CD, Barker GJ, et al. **Sensitivity of contrast enhanced MRI in multiple sclerosis: effects of gadolinium dose, magnetization transfer contrast and delayed imaging.** *Brain* 1997;120(Pt 7):1149–1161
40. Koenig SH. **Cholesterol of myelin is the determinant of gray-white contrast in MRI of brain.** *Magn Reson Med* 1991;20:285–291
41. Koenig SH, Brown RD, Spiller M, Lundbom N. **Relaxometry of brain: why white matter appears bright in MRI.** *Magn Reson Med* 1990;14:482–495
42. Ceckler TL, Wolff SD, Simon A, Yip V, Balaban RS. **Dynamic and chemical factors affecting water proton relaxation by macromolecules.** *J Magn Reson* 1992;98:637–645
43. Kucharczyk W, Macdonald PM, Stanisz GJ, Henkelman RM. **Relaxivity and magnetization transfer of white matter lipids in MR imaging: importance of cerebrosides and pH.** *Radiology* 1994;192:521–529
44. Koller KJ, Zaczek R, Coyle JT. ***N*-acetyl-aspartyl glutamate: regional levels in rat brain and the effects of brain lesions as determined by a new HPLC method.** *J Neurochem* 1984;43:1136–1142
45. Coyle JT, Robinson MB, Blakely RD, Forloni GL. **The neurobiology of *N*-acetyl-aspartyl glutamate.** In: *Allosteric Modulation of Amino Acid Receptors: Therapeutic Implications.* New York: Raven Press; 1989:319–333
46. Gill SS, Small RK, Thomas DG, et al. **Brain metabolites as 1H NMR markers of neuronal and glial disorders.** *NMR Biomed* 1989;2:196–200
47. Matthews PM, Francis G, Antel J, Arnold DL. **Proton magnetic resonance spectroscopy for metabolic characterization of plaques in multiple sclerosis.** *Neurology* 1991;41:1251–1256
48. Arnold DL, Matthews PM, Francis GS, O'Connor J, Antel JP. **Proton magnetic resonance spectroscopic imaging for metabolic characterization of demyelinating plaques.** *Ann Neurol* 1992;31:235–241
49. Preece NE, Butter C, Gadian DG, Urenjak J, Baker D. **1H-NMR studies of CNS metabolism in a guinea pig model of multiple sclerosis.** In: *Proceedings of the Tenth Annual Meeting of the SMRM.* San Francisco: Society of Magnetic Resonance in Medicine; 1991:432
50. De Stefano N, Matthews PM, Arnold DL. **Reversible decreases in *N*-acetylaspartate after acute brain injury.** *Magn Reson Med* 1995;34:721–727
51. De Stefano N, Matthews PM, Antel JP, Preul M, Francis G, Arnold DL. **Chemical pathology of acute demyelinating lesions and its correlation with disability.** *Ann Neurol* 1995;38:901–909
52. Hiehle JF Jr, Lenkinski RE, Grossman RI, et al. **Correlation of spectroscopy and magnetization transfer imaging in the evaluation of demyelinating lesions and normal appearing white matter in multiple sclerosis.** Magn Reson Med 1994;32:285–293
53. Kimura H, Grossman RI, Lenkinski RE, Gonzalez-Scarano F. **Proton Mr spectroscopy and magnetization transfer ratio in multiple sclerosis: correlative findings of active versus irreversible plaque disease.** *AJNR Am J Neuroradiol* 1996;17:1539–1547
54. Kurtzke JF. **Rating neurologic impairment in multiple sclerosis: An expanded disability status scale.** *Neurology* 1983;33:1444–1452
55. Poser CM, Paty DW, Scheinberg L, et al. **New diagnostic criteria for multiple sclerosis: guidelines for research protocols.** *Ann Neurol* 1983;13:227–231

56. Ordidge RJ, Mansfield P, Prime JAL. **Volume selection using gradients and selective pulses.** *Ann N Y Acad Sci* 1987;508:376–385
57. den Hollander JA, Oosterwal B, Vroonhoven HV, Luyten PR. **Elimination of magnetic field distortions in 1H NMR spectroscopic imaging.** In: *Proceedings of the Society of Magnetic Resonance in Medicine.* San Francisco: Society of Magnetic Resonance in Medicine; 1991:472
58. Davies SE, Newcombe J, Williams SR, McDonald WI, Clark JB. **High resolution proton NMR spectroscopy of multiple sclerosis lesions.** *J Neurochem* 1995;64:742–748
59. Husted CA, Goodin DS, Hugg JW, et al. **Biochemical alterations in multiple sclerosis lesions and normal-appearing white matter detected by in vivo 31p and 1H spectroscopic imaging.** *Ann Neurol* 1994;36:157–165
60. Pan JW, Hetherington HP, Vaughan JT, Mitchell G, Pohost GM, Whitaker JN. **Evaluation of multiple sclerosis by 1H spectroscopic imaging at 4.1 T.** *Magn Reson Med* 1996;36:72–77
61. Kamber M. ***Automated Detection of Multiple Sclerosis Lesions in Magnetic Resonance Images of the Human Brain.*** Concordia University; 1991. Thesis
62. Collins DL, Neelin P, Peters TM, Evans AC. **Automatic 3D intersubject registration of MR volumetric data in standardized talairach space.** *J Comput Assist Tomogr* 1994;18:192–205
63. Loevner LA, Grossman RI, Cohen JA, Lexa FJ, Kessler D, Kolson DL. **Microscopic disease in normal-appearing white matter on conventional MR images in patients with multiple sclerosis: assessment with magnetization-transfer measurements.** *Radiology* 1995;196:511–515
64. Filippi M, Campi A, Dousset V, et al. **A magnetization transfer imaging study of normal appearing white matter in multiple sclerosis.** *Neurology* 1995;45(Pt 1):478–482
65. Lexa FJ, Grossman RI, Rosenquist AC. **MR of wallerian degeneration in the feline visual system: characterization by magnetization transfer rate with histopathologic correlation.** *AJNR Am J Neuroradiol* 1994;15:201–212
66. Mehta RC, Pike GB, Enzmann DR. **Magnetization transfer MR of the normal adult brain.** *AJNR Am J Neuroradiol* 1995;16:2085–2091
67. Barnes D, Munro PM, Youl BD, Prineas JW, McDonald WI. **The longstanding MS lesion: a quantitative MRI and electron microscopic study.** *Brain* 1991;114(Pt 3):1271–1280
68. Pike GB, De Stefano N, Narayanan S, Francis G, Antel J, Arnold DL. **A longitudinal study of magnetization transfer in multiple sclerosis.** In: *Proceedings of the International Society for Magnetic Resonance in Medicine.* Sydney, Australia: International Society for Magnetic Resonance in Medicine; 1998:122
69. Filippi M, Paty DW, Kappos L, et al. **Correlations between changes in disability and T2-weighted brain.** *Neurology* 1995;45:255–260
70. Gasperini C, Horsfield MA, Thorpe JW, et al. **Macroscopic and microscopic assessments of disease burden by MRI in multiple sclerosis: relationship to clinical parameters.** *J Magn Reson Imaging* 1996;6:580–584
71. Paty DW, Li DK. **Interferon beta-1b is effective in relapsing-remitting multiple sclerosis: ii: MRI analysis results of a multicenter, randomized, double-blind, placebo-controlled trial: UBC MS/MRI study group and the IF NB multiple sclerosis study group (comments).** *Neurology* 1993;43:662–667
72. Henkelman RM, Huang X, Xiang QS, Stanisz GJ, Swanson SD, Bronskill MJ. **Quantitative interpretation of magnetization transfer.** *Magn Reson Med* 1993;29:759–766